International Conference on the Technology of Plasticity, ICTP 2017, 17-22 September 2017, Cambridge, United Kingdom

Shear forming of 304L stainless steel – microstructural aspects

M. Guillot[a],*, T. McCormack[b], M. Tuffs[b], A. Rosochowski[a], S. Halliday[b], P. Blackwell[a]

[a]*University of Strathclyde, 75 Montrose Street, Glasgow G1 1XJ, United-Kingdom*
[b]*Rolls-Royce, PO Box 31, Derby DE24 8BJ, United-Kingdom*

Abstract

Shear forming is an incremental cold forming process. It transforms 2D plates into 3D structures commonly consisting of conical geometry. Roller(s) push the blank onto a cone-shaped mandrel, resulting in a decrease of the initial thickness. The shear forming process has diverse advantages, such as improved material utilisation, enhanced product characteristics, good surface finish, consistent geometric control and reduced production costs. Shear forming has potential applications in a wide range of conical geometries used within advanced aerospace structures, which are currently manufactured from bulk forgings with high associated machining costs.

Research findings related to shear forming have been published over the past two decades, however, important remaining questions have still to be answered, with this paper addressing one such gap associated with the material deformation mechanism. Several studies have demonstrated the impact of key process variables on the final geometry and surface roughness, such as the feeds, roller nose radius and mandrel/roller offset. Although the material outputs are essential, as they link directly with the mechanical properties of the final components, the microstructure and texture of the material after shear forming have rarely been studied. Achieving a greater understanding in this area could reduce the reliance upon mechanical testing to validate the process and ease the exploitation route of the technology into advanced aerospace applications.

Firstly, this paper presents the principle of shear forming and its related terminology. Then, a brief overview of the shear forming process including its history and origin is given. The areas of focus are a selection of the main variables encountered within this process which could impact the final properties. The generation of local stresses due to deviations from the sine law, the angle variations, and forces required during the forming operation are also considered. This is explored in the context of forming 304L stainless steel plates.

* Corresponding author.
E-mail address: marine.guillot@strath.ac.uk

This paper is written based upon experiments which observed a 52% thickness reduction using one roller. Scanning Electron Microscopy (SEM), Electron BackScatter Diffraction (EBSD) and hardness testing were utilised to characterise the shear formed material. The initial heterogeneous microstructure with relatively equiaxed grains evolved into a microstructure with elongated grains along with shear bands. A texture analysis revealed a simple shear mechanism of deformation, and theoretical and experimental shears were found to match.

Identifying the mechanism of deformation was the first step to a better understanding of the effect imparted by the shear forming process on the material. Further studies will look at the impact of the key process variables on both the microstructure and texture as well as heat treatment optimisation.

1. Introduction

Shear forming is also known as flow forming, shear spinning, shear turning, power spinning, or spin forging. It is an incremental cold forming process which manufactures rotationally symmetrical conical, concave, or convex hollow profiled engineering components. Minimal waste and a dimensional accuracy similar to that of machined components are obtained using today's CNC flow formers. Shear forming should not be mistaken for conventional spinning, as the latter combines tension and compression of the material without intentional thickness reduction of the starting blank. Conversely, shear forming involves only compression forces and reduces the initial material thickness [1]. Although spinning methods were born with the art of potting clay in ancient Egypt [2], the first papers mentioning shear forming were published 60 years ago and its expansion has mainly occurred over the past two decades.

Fig. 1 describes shear forming's three operational steps: 1. a flat circular blank is clamped against a mandrel by a tailstock; 2. the mandrel is rotated; 3. one or more rollers then force the blank to incrementally take the shape of the mandrel by following a programed path using a controlled feed rate. Generally, only a single pass is required to produce the final shape but multiple passes can be undertaken to enhance dimensional control.

The final thickness of the part, S_1, is determined from the sine law (Equation 1), where α is the angle of the mandrel and S_0 the initial blank thickness. The key impact of the sine law is that a small angle α will produce a smaller thickness S_1, requiring larger levels of deformation. As such, the minimum angle of the mandrel possible to shear form is in the range 10 to 18°, dependent on the material being formed; smaller angles as low as 3 to 4°, however, can be achieved using multiple passes [1]. Deviations from the sine law are sometimes observed and lead to failure or defects in the part, which are due to induced stress, a phenomenon directly noticeable on the flange of the workpiece. Material build-up is one of the main causes of deviation and can be prevented by using more rollers and/or multiple passes [3].

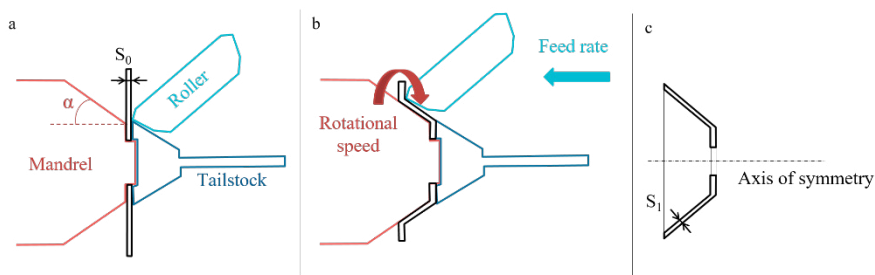$$S_1 = S_0 \cdot sin(\alpha) \tag{1}$$

Fig. 1. Shear forming principle: (a) Set-up; (b) In operation; (c) Part completed.

During shear forming, axial, radial, and tangential forces are generated between the blank and the roller, out of which the tangential force is usually found to be the smallest. Multiple researchers have attempted to calculate the latter by considering shear deformation or a combination of shear deformation and bending strain. In 2001, Chen et

al. [4] linked these forces to the process variables and in 2003, Kim et al. [5] obtained convergence of experimental and theoretical tangential forces by considering a pure shear model. Understanding the forces required to shear form a blank is essential to define the limitations of such a process and this involves understanding the material behavior as well as the effect of process parameters. Although Zhan et al. [6] and Radović et al. [7] studied the microstructure and texture of shear formed components made of Al and Al-Mg alloys, the material deformation mechanism was not identified. Common materials currently industrially shear formed are steel, copper, aluminum, and nickel, plus a much wider range of materials have been successfully shear formed in laboratory trials [1]. Potential future applications include a wide spectrum of conical structures used in gas turbine engines, aerospace structures and military equipment.

2. Experimental set-up

The material used in this study was a 6 mm thick 304L stainless steel sheet that had been hot rolled, solution annealed, and pickled in accordance with the standard EN 10088-2. Its chemical composition and mechanical properties are given by Tables 1 and 2 respectively. Prior to shear forming, the blanks were water jet cut with an external diameter of 430 mm and an internal diameter of 150 mm.

Table 1. Chemical composition (% by mass) of the as-received sheet.

C	Cr	Mn	N	Ni	P	S	Si
0.018	18.050	1.773	0.067	8.035	0.031	0.002	0.449

Table 2. Mechanical properties of the as-received sheet.

Ultimate tensile strength	Yield strength at		Elongation after fracture		Vickers hardness
	0.2%	1%	A50	A5	
635 N/mm²	348 N/mm²	391 N/mm²	52 %	53 %	186 HV1

Shear forming experiments were carried out at the Advanced Forming Research Centre (AFRC) – University of Strathclyde, using a WF Maschinenbau 3-roller-flow forming and spinning machine of the type STR 600 3/6 pictured in Fig. 2 (a). One 3 mm nose radius roller was utilised to shear form the blanks onto a mandrel with a 31.5° angle, which according to the sine law corresponds to a thickness reduction of 52%. The resultant geometrical transformation is shown by Fig. 2 (b). During the process, the surface speed and feed rate were held constant at 480 m/min and 1.0 mm/rev respectively. An oil-based coolant, Houghton Hocut 795B, was employed at a flow rate of 400 L/min.

Five specific areas of interest taken from a cross-sectional slice of the final parts, identified by Fig. 2 (c), were then analysed using Scanning Electron Microscopy (SEM) and Electron BackScattered Diffraction (EBSD), with a microscope type FEI Quanta 250 FEG. Hardness tests were performed using a micro-hardness tester of type Zwick-Roell Indentec ZHμ, at 1 kg force. The measurements were made in accordance with the ISO 6507-1 standard. The level of confidence in the results was of 95%. The values taken into account for this study are an average of the three indents across the thickness of the sample.
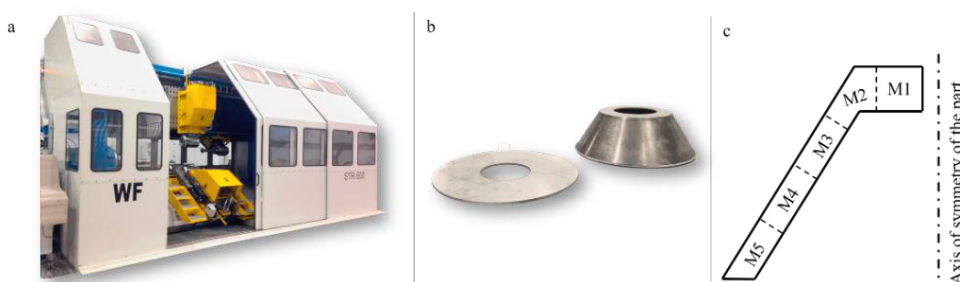

Fig. 2. (a) Flow former; (b) Blank and shear formed part; (c) Areas of metallurgical interest.

Micrographs were taken in BackScatter (BS) mode. The coordinate systems adopted for reporting the microstructural data of area M1 were the rolling direction (RD), transverse direction (TD) and normal direction (ND) whereas the cylindrical coordinates (R, θ, Z) were used for the remaining areas. The texture was analysed by EBSD with a step size of 1.0 and 0.3 µm for the as-received and shear formed areas respectively. Pole Figures (PFs) and Orientation Distribution Functions (ODFs) were displayed using the settings given by Tables 3 and 4.

Table 3. Settings employed to generate the PFs.

Half width	Cluster size	Coordinate system	Projection type	Projection hemisphere	Planes	Colours	Contour lines
10°	5°	R, θ, Z	Stereographic	Upper	{100}, {110}, {111}	Max. intensity at 6	Step width of 1.5 Max. at 6

Table 4. Settings employed to generate the ODFs.

Half width	Cluster size	Coordinate system	Colours	Contour lines	Sample symmetry	Method	Resolution	Calculation
Gaussian, 5°	5°	R, θ, Z	Rainbow	At 2, 4, 6, 8, and 10	Triclinic	Gaussian estimation	128x32x32	Based on full map

3. Results and discussion

Fig. 3 shows the micrographs of the part in the different areas of interest. From EBSD analysis it was estimated that the as-received material, represented by area M1, had approximately equiaxed grains with an average grain size of 11.3 µm (ASTM 9.5-10) with 70% of the grains being under or equal to 10.0 µm. The initial material was heterogeneous and had a relatively weak rolling texture.
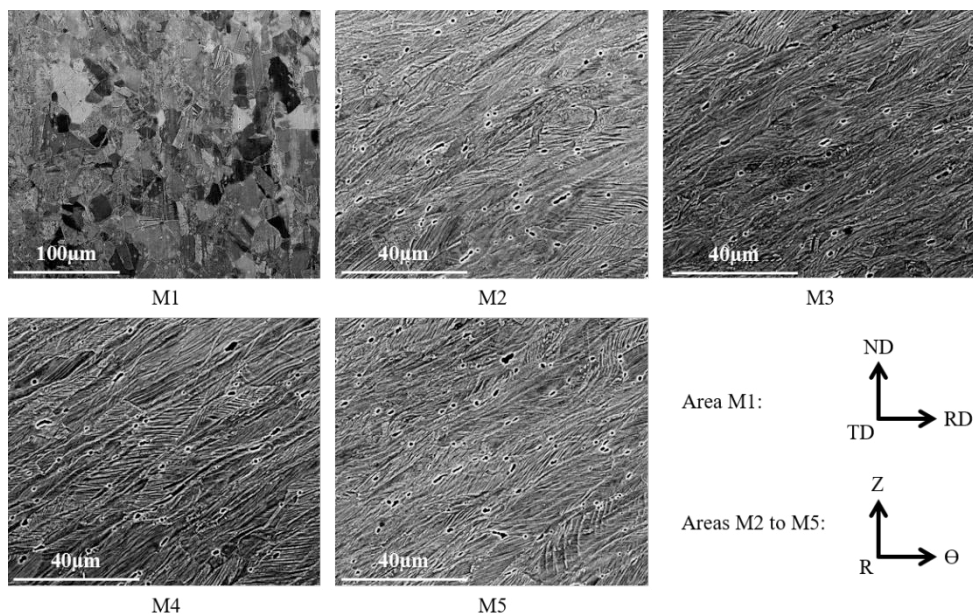

Fig. 3. Micrographs along the shear formed part.

The shear formed areas, M2 to M5, presented elongated grains and only slight microstructural differences were noticed. Shear bands representative of high local deformation during plastic deformation were observed. They presented primary orientations along the θ axis of the cylindrical coordinates and slightly tilted from the shear forming direction. These aligned shear bands were ascertained with a principal spacing around 1 µm. Simple shear, a specific

mechanism of deformation, is detected when one direction of the initial material which is free to rotate on both ends remains constant and everything else rotates relative to it. Fig. 4 (a) illustrates this phenomenon with the transformation of a square to a rhombus along with the rotation of the ellipsoid axes from their original position, which is another characteristic of simple shear. This mechanism was identified on the BS images of Fig. 3 (areas M2 to M5) where elongation of the grains and shear bands along the main ellipsoid axis are shown. Although the actual stress-strain state in the material can be significantly triaxial and complex, the model of the process can be simplified assuming that at each contact between the roller and material only elementary simple shear takes place. In this case, the intensity of this shear, γ, can be estimated as α tangent. Fig. 4 (b) is the plot of the shear as a function of the angle of the mandrel. The shear for the current geometry was about $\gamma=1.6$.

An EBSD map was acquired in the middle of the thickness of area M4 and an austenite to martensite transformation was observed. The PFs are given by Fig. 5. According to the Kurdjumov-Sachs orientation relationship, the plane $\{111\}_{fcc}$ is parallel to $\{110\}_{bcc}$. This can be seen in these specific PFs as they show the same elements in identical areas, which is characteristic of shear transformation. This transformation of austenite to martensite was also proved by the part becoming magnetic. By comparing the PF $\{111\}_{fcc}$ with the PFs presented by Barnett et al. [8], an equivalent strain of about 1.7 was identified. Few of the main torsion texture components, which are defined in Fig. 6, were noticed on the PFs $\{111\}$.

To look at this deformation in more detail, ODFs were calculated. In the case of simple shear deformation, the specific components B and $\bar{B}$ are identified on ODFs displayed at $\Phi=55°$ and $\Phi_2=45°$. They are generally observed for these settings at $\Phi_1=0, 120, 240°$ and $\Phi_1=60, 180, 300°$ for B and $\bar{B}$ respectively [9]. The ODFs of both fcc and bcc phases are given by Fig. 5. In both cases, the components B and $\bar{B}$ were identified whereas the components A_1^*, A_2^* and C only appeared clearly for the fcc phase. According to these results, the mechanism of deformation was simple shear.
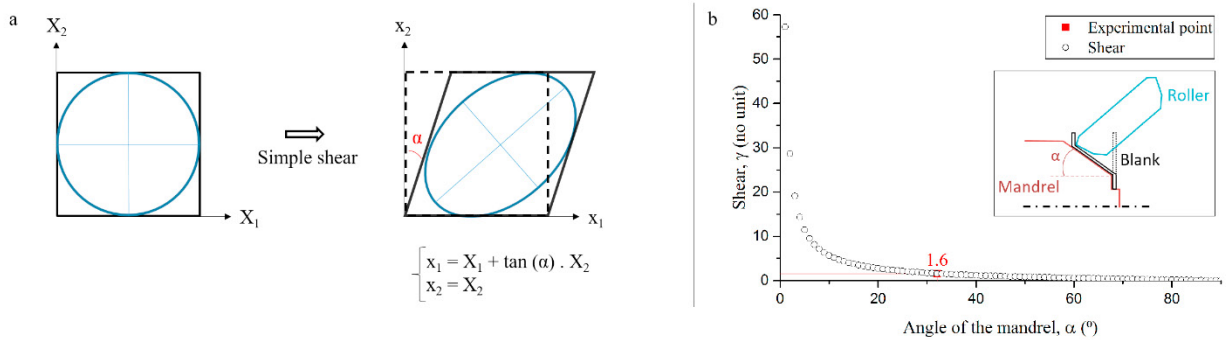

Fig. 4. Simple shear: (a) Illustration of the principle; (b) Plot of the shear as a function of the angle of the mandrel.
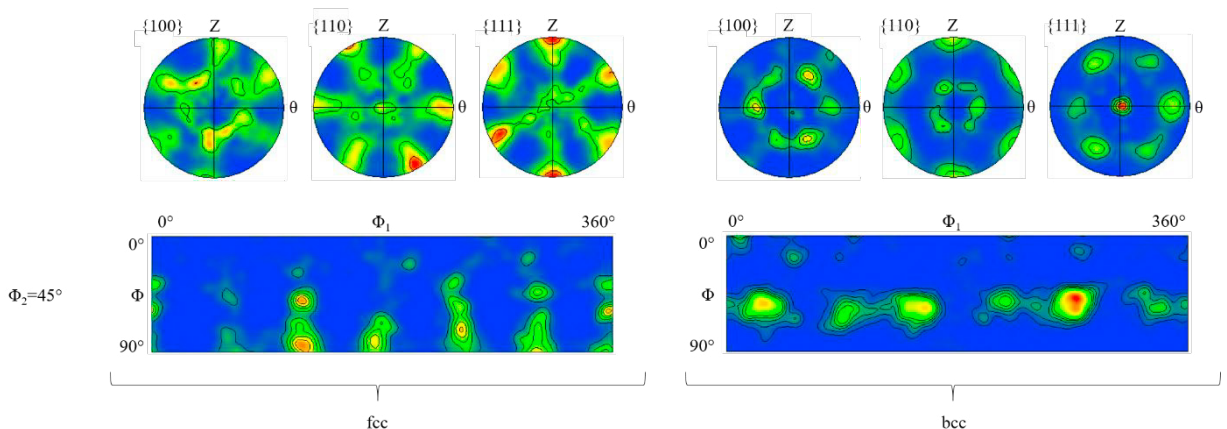

Fig. 5. Texture representations for the middle of the thickness of area M4 (top: PFs; bottom: ODFs).

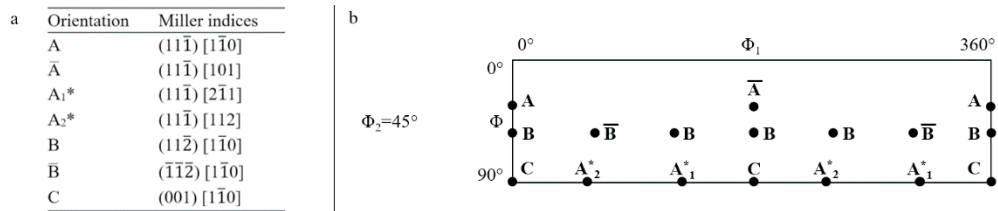| a	Orientation	Miller indices
	A	$(11\bar{1})[1\bar{1}0]$
	$\bar{A}$	$(11\bar{1})[101]$
	A_1^*	$(11\bar{1})[2\bar{1}1]$
	A_2^*	$(11\bar{1})[112]$
	B	$(11\bar{2})[1\bar{1}0]$
	$\bar{B}$	$(\bar{1}\bar{1}2)[1\bar{1}0]$
	C	$(001)[1\bar{1}0]$

Fig. 6. Main torsion texture components: (a) Miller indices; (b) Representation on ODFs.

Some low-force hardness tests were performed to see if the hardness changed across the part. The results for area M1, considered as the as-received material, met the data given by the material certificate in Table 2. The outcomes showed a variation within the part of 5HV1 in the shear formed areas, which suggests that the microstructure is reasonably homogeneous in this area, as is borne out in Fig. 3. The highest hardness values were recorded at the transition of as-received and shear formed areas with 370HV1.

4. Conclusions

The initial material with relatively equiaxed grains evolved to a structure with elongated grains after being shear formed. Its hardness doubled during the process to reach values around 370HV1. High local deformation was observed in the form of shear bands along the θ axis of the cylindrical coordinates and slightly titled from the shear forming direction. Micrographs and hardness analysis showed a homogeneous microstructure along the shear formed length of the part. A transformation of austenite to martensite was observed, which was proved in practice by the part becoming magnetic. The main mechanism of deformation was identified as simple shear thanks to experimental and theoretical shears and identification of the main torsion texture components on the PFs and ODFs for both fcc and bcc phases of the material.

Shear forming has a clear effect on the microstructure, hardness and texture of the material. The effect of process parameters on the resulting material characteristics of the formed component is of great relevance to this technology and further studies should explore this area. Also planned are detailed assessments across the thickness of shear formed parts to establish the existence of any gradient. These are important considerations which should be included at the early design stage of any engineering component shaped by shear forming.

Acknowledgements

References

[1] M. Runge, Spinning and flow forming, Leifeld GmbH, Ahlen, 1993.
[2] C.C. Wong, T.A. Dean, J. Lin, A review of spinning, shear forming and flow forming processes, Int. J. Mach. Tools Manuf. 43 (2003) 1419-1435.
[3] O. Music, J.M. Allwood, K. Kawai, A review of the mechanics of metal spinning, J. Mater. Process. Techno. 210 (2010) 3-23.
[4] M.D. Chen, R.Q. Hsu, K.H. Fuh, Forecast of shear spinning force and surface roughness of spun cones by employing regression analysis, Int. J. Mach. Tools Manuf. 41 (2001) 1721-1734.
[5] C. Kim, S.Y. Jung, J.C. Choi, A lower upper-bound solution for shear spinning of cones, Int. J. Mech. Sci. 45 (2003) 1893-1911.
[6] M. Zhan, X. Wang, H. Long, Mechanism of grain refinement of aluminium alloy in shear spinning under different deviation ratios, Mater. Des. 108 (2016) 207-216.
[7] L. Radović, M. Nikačević, B. Jordović, Deformation behaviour and microstructure evolution of AlMg6Mn alloy during shear spinning, Trans. Nonferrous Met. Soc. China 22 (2012) 991-1000.
[8] M.R. Barnett, F. Montheillet, The generation of new high-angle boundaries in aluminium during hot torsion, Acta Materialia 50 (2002) 2285-2296.
[9] M.M.Z. Ahmed, The development of thick section welds and ultra-fine grain aluminium using friction stir welding and processing, University of Sheffield, 2009.